Published in final edited form as:
J Cell Sci. 2008 August 1; 121(Pt 15): 2493–2502. doi:10.1242/jcs.025528.

Laminin α5 influences the architecture of the mouse small intestinal mucosa

Zhen X. Mahoney[1], **Thaddeus S. Stappenbeck**[2], and **Jeffrey H. Miner**[1,3,*]

1*Department of Internal Medicine/Renal Division, Washington University School of Medicine, St. Louis, MO 63110, USA*

2*Department of Pathology and Immunology, Washington University School of Medicine, St. Louis, MO 63110, USA*

3*Department of Cell Biology and Physiology, Washington University School of Medicine, St. Louis, MO 63110, USA*

Summary

The mammalian intestine displays two distinct patterns of mucosal organization. The small intestine contains mucosal epithelial invaginations called crypts of Lieberkühn that are continuous with evaginations into the lumen called villi. The colon also contains crypts, but its epithelial surface is lined by flat surface cuffs. The epithelial cells of both organs communicate with the underlying mesenchyme through a basement membrane that is composed of a variety of extracellular matrix proteins, including members of the laminin family. The basement membranes of the small intestine and colon contain distinct laminin subtypes; notably, the villus basement membrane is rich in laminin α5. Here we show that diminution of laminin α5 in a mouse model led to a compensatory deposition of colonic laminins that resulted in a transformation from a small intestinal to a colonic mucosal architecture. The alteration in mucosal architecture was associated with reduced levels of nuclear $p27^{Kip1}$, a cell cycle regulator, and altered intestinal epithelial cell proliferation, migration, and differentiation. Our results suggest that laminin α5 plays a crucial role in establishing and maintaining the specific mucosal pattern of the mouse small intestine.

Keywords

basement membrane; small intestine; intestinal epithelial cell; Lutheran; $p27^{Kip1}$

INTRODUCTION

The mouse and human gastrointestinal tubes are divided into stomach, small intestine, and colon. In each of these organs, the inner mucosal surface is composed of a continuous simple epithelium that is in contact with both the lumen and the underlying mesenchymal components, including blood vessels, myofibroblasts and immune cells, which collectively form the lamina propria. At the base of the mucosa is a thin layer of smooth muscle, the muscularis propria. Each organ establishes a specific mucosal organization that is critical to the function of that particular organ. For example, to increase its absorptive surface, the small intestine contains a multitude of finger-like structures, called villi, that project into the lumen. Villi are covered by an epithelium that is supplied by 4-8 adjacent pit-like invaginations called crypts of Lieberkühn.

*Address correspondence to: Jeffrey H. Miner, Washington University School of Medicine, Renal Division, Box 8126, 660 S. Euclid Ave., St. Louis, MO 63110, 314-362-8235 (Tel), 314-362-8237 (Fax), minerj@wustl.edu.

In contrast, the absorptive load of the colonic mucosa is far less than that of the small intestine, and it contains no villi. Colonic crypts supply the relatively flat surface epithelium (Sancho et al., 2004). It is not well understood how the gastrointestinal tube develops and maintains specific mucosal patterns along the cephalocaudal axis.

The epithelium of the intestinal mucosa undergoes rapid and perpetual renewal throughout life (reviewed in Sancho et al., 2004; Radtke and Clevers, 2005). In the small intestine, epithelial stem cells reside near the base of crypts and give rise to epithelial progenitor cells (Potten et al., 1997; Booth and Potten, 2000). Epithelial progenitor cells are transit-amplifying cells, which exit the cell cycle at the junction of crypts and villi and differentiate into four distinct cell types. Three of these cell types, the absorptive enterocytes, the mucus-secreting goblet cells and the hormone-secreting enteroendocrine cells, complete their differentiation as they migrate upwards onto adjacent villi in an ordered column. These three cell types reach the villus tip in two to five days and undergo programmed cell death and sloughing into the intestinal lumen. In contrast, Paneth cells, the fourth cell type, migrate downwards to the base of the crypts while completing terminal differentiation. The epithelium of the mouse colon is organized similarly, except that villi and Paneth cells are not present. Colonic epithelial cells complete terminal differentiation during migration through the upper crypt and onto the flat epithelial surface (Stappenbeck et al., 1998; Radtke and Clevers, 2005).

At the interface of the epithelium and lamina propria lies a thin sheet of specialized extracellular matrix, the basement membrane (BM). BMs are widely distributed in the body, surrounding all epithelia, endothelia, muscles, nerves, and fat cells (Kalluri, 2003). Besides a structural role in maintaining tissue integrity and compartmentalization, BMs also promote cell adhesion, survival, proliferation, differentiation, and serve as a highway for cell migration. Laminin, type IV collagen, nidogen, and sulfated proteoglycans are the four main components of all BMs (Timpl, 1996; Timpl and Brown, 1996). Laminins are αβγ heterotrimers formed from a family of five α, four β, and three γ chains that can assemble into at least 15 unique isoforms (Miner and Yurchenco, 2004). In vitro studies show that different laminin isoforms exhibit different properties in terms of regulating cell adhesion, proliferation, differentiation and migration (Vachon and Beaulieu, 1995; Siler et al., 2000; Pouliot et al., 2002; Turck et al., 2005). Distinct phenotypes from various laminin chain knockouts also indicate a functional divergence among laminins (Yurchenco et al., 2004). The distribution of laminin isoforms within tissues is tightly controlled and often developmentally regulated (Miner, 1998; Simon-Assmann et al., 1998; Lefebvre et al., 1999). The functional implications of such a wide and dynamic distribution of laminin isoforms in tissues have only begun to be explored.

With regard to the intestine, a large number of studies over the last two decades using cell culture models have attempted to address the roles of individual extracellular matrix molecules in regulating intestinal cell behavior (Simon-Assmann et al., 2007). Although much important progress has been made, the lack of a bona fide BM and the proper cellular and vascular microenvironments in most cases leads to questions regarding applicability to the in vivo situation. Here we report the generation of mutant mice that lack the laminin α5 chain, and thus the laminin α5β1γ1 trimer (LM-511 in the new nomenclature; Aumailley et al., 2005), in the intestinal subepithelial BM in vivo. This resulted in a shift of the laminins in the villus BM to the colonic type isoforms (LM-111 and LM-411), which caused a colonic transformation of the mutant small intestine. These data reveal that the specific combinations of laminin isoforms that are deposited in the subepithelial BM contribute to patterning the intestinal tube into small intestine and colon. We further demonstrated that laminins are instructive for pattern formation by influencing intestinal epithelial cell behavior, likely through $p27^{Kip1}$, a cell-cycle regulator that is also involved in regulating differentiation, migration, and apoptosis.

RESULTS

A laminin α5 transgene widely expressed during embryonic development is silenced in adult mouse small intestinal mucosa

Lama5$^{-/-}$ mice die in late gestation, exhibiting growth retardation and multiple developmental defects (Miner et al., 1998; Miner and Li, 2000; Nguyen et al., 2002; Bolcato-Bellemin et al., 2003; Fukumoto et al., 2006; Rebustini et al., 2007). Defective placental vascularization is likely the defect that causes embryonic lethality (Miner et al., 1998), which has hindered further study of the roles of laminin α5 in vivo beyond fetal development. Previously we produced two independent lines of transgenic mice expressing a full-length mouse laminin α5 transgene (called Mr5; see Fig. 1A). Miw, the regulatory element used, contains a Rous sarcoma virus long terminal repeat inserted into the chicken β-actin promoter, a combination that is widely active in transgenic mice (Suemori et al., 1990). The Mr5 transgene in both lines directs widespread deposition of full length laminin α5 in BMs such that transgene-derived protein rescues all known developmental defects of *Lama5*$^{-/-}$ mice (Kikkawa and Miner, 2006). Thus, during embryonic development, transgene-derived laminin α5 accumulates in BMs wherever it is necessary, and it is functional, such that *Lama5*$^{-/-}$; Mr5 (KO/Tg) mice are viable and fertile.

While surveying the deposition pattern of Mr5-derived protein in postnatal KO/Tg animals, we discovered that levels were low in the small intestine, kidney and lung (Fig. 1 and data not shown). In contrast to the abundant laminin α5 staining in control *Lama5*$^{+/-}$; Mr5 (Het/Tg) mice, which are phenotypically indistinguishable from wild-type mice (Fig. S1 and data not shown), α5 levels were greatly reduced in the villus subepithelial BM throughout the length of the KO/Tg small intestine. The reduction was first obvious around one month of age, and most of the laminin α5 was lost in mice over three months of age (n=32) (Fig. 1D-I). This reduction was confirmed by three additional antibodies recognizing distinct epitopes along the α5 protein (data not shown). Interestingly, KO/Tg small intestines did contain laminin α5 in mesenchymal structures within the villi and in the intestinal smooth muscle at all ages (Fig. 1D-I).

The observed reduction in α5 levels was consistent in over forty KO/Tg mice examined from both independent lines. Furthermore, in an unrelated transgenic line in which fatty acid transport protein 4 was expressed under the same Miw regulatory element present in Mr5, transgene-derived protein was also greatly reduced in the adult small intestine ((Moulson et al., 2007) and data not shown). To investigate whether laminin α5 was reduced at the mRNA level, we performed quantitative real-time RT-PCR and found that laminin α5 mRNA was greatly diminished in KO/Tg intestinal epithelial cells and mucosa (Table 1). Together, these data demonstrate that after embryonic development, the expression of the Mr5 transgene wanes, leading to the eventual loss of α5 from the intestinal epithelial BM.

Laminin α5 is required for both establishing and maintaining small intestinal crypt-villus architecture

The reduction of laminin α5 in the subepithelial BM during postnatal life led to dramatic changes in the architecture of the small intestinal mucosa. Whole-mount analysis of Het/Tg and KO/Tg small intestine showed that the normally slender, finger-shaped individual villi (Fig. 2A) appeared to coalesce to varying degrees in the KO/Tg small intestine. These alterations included what appears to be simple fusion of adjacent villi (Fig. 2B), fusion of multiple consecutive villi in a “cerebroid” pattern (Fig. 2C), and complete loss of individual villi in a “mosaic” pattern (Fig. 2D). The latter strongly resembles the surface of the mouse colon (Fig. 3H). This abnormal mucosal structure was also apparent by scanning electron microscopy (Fig. 2E-G).

The villus coalescence first appeared in the distal small intestine, but spread to proximal and middle small intestine segments in mice of advanced age (Fig. S2). No apparent changes in the colon were observed (Fig. S2), despite the fact that laminin α5 was also reduced in KO/Tg colon with concomitant upregulation of laminin α1 (Fig. S1). It is not clear why the distal small intestine suffered more severe villus fusion compared to the more proximal parts, despite the fact that α5 levels were greatly reduced throughout the length of the KO/Tg small intestine (Fig. 1). In the following studies we chose to focus on the distal small intestine, as it displayed an early-onset and consistent phenotype. In the distal small intestine, signs of villus coalescence were first observed around two months of age (4 out of 5 mice), and a more advanced stage of villus coalescence (the "cerebroid" pattern) occurred in mice at least nine months of age (23 out of 23 mice). At the same age, female mice tended to exhibit a more severe phenotype than male mice. All mice were maintained on a mixed 129-C57BL/6J-CBA/J background.

To gain a better understanding of the basis for villus coalescence, we carefully obtained histological sections perpendicular (Fig. 3A-D) or parallel (Fig. 3E,F) to the intestinal muscle wall. The histology of KO/Tg sections correlated with the findings in whole mount views and, in addition, revealed extended crypts between joined villi (Fig. 3B,C,F). In severe cases of villus coalescence, the deep-crypt, flat surface epithelium architecture in KO/Tg distal small intestine (Fig. 3C) largely resembled a colon (Fig. 3D). Thus, following the reduction of laminin α5 levels, the KO/Tg small intestine gradually loses the crypt-villus architecture of a normal small intestine and adopts a colon-like structure. Our data suggest that laminin α5 is required for the maintenance of a normal small intestine pattern in adult mice. One point worth noting here is that because villus coalescence seems to occur in a linear zigzag fashion (Fig. 2C,F; Fig. S2), in two-dimensional sections perpendicular to the intestinal wall, the majority of villi appear to be unfused, even though in three-dimensional whole-mount views the majority of villi are fused.

We next asked whether laminin α5 was also required to establish a normal small intestine pattern, rather than to merely maintain it. To address this question, we studied embryonically lethal *Lama5*$^{-/-}$ mice. To overcome the problem that small intestinal crypt-villus structure is not established until one month after birth, we grafted intestines from *Lama5*$^{-/-}$ and control embryos under the dorsal skin of nude mice. After one month, control small intestine grafts developed a typical crypt-villus architecture (Fig. 3I). However, the *Lama5*$^{-/-}$ small intestine graft developed an abnormal crypt-villus architecture (Fig. 3J) and, in severe cases (Fig. 3K), resembled a grafted normal colon (Fig. 3L). Combining the data from both *Lama5*$^{-/-}$ mice and KO/Tg mice, we conclude that laminin α5 is required for both the establishment and maintenance of small intestinal crypt-villus architecture.

KO/Tg distal small intestine undergoes colonic transformation

The architectural resemblance between the distal small intestine of KO/Tg mice and the colon of wild-type mice prompted us to determine whether there was any additional evidence that this alteration was a transformation of one tissue type (small intestine) into another (colon). To do this we examined the subtypes of mucin secreted by goblet cells. A transition in mucin subtypes has been used in diagnosing colonic transformation in patients (Mimura et al., 1999; Di Tonno et al., 2001). In mice, sulfomucin-containing goblet cells are predominant in the small intestine, whereas those containing sialomucin are only found in the colon (Deplancke et al., 2000). These two subtypes can be readily distinguished by high iron diamine staining, which stains sialomucin blue and sulfomucin brown. We observed a substantial number of sialomucin-containing goblet cells in the KO/Tg distal small intestine, even in areas without the dramatic crypt-villus architecture changes noted above (n=4) (Fig. 4A-C).

Transmission electron microscopic analysis revealed additional evidence of colonic transformation. Goblet cells in the normal Het/Tg small intestine contained small (1.2 μm

diameter on average; 20 granules from two mice were measured) electron-dense granules (Fig. 4D), whereas goblet cells in the KO/Tg small intestine contained larger (2.2 μm diameter on average; 20 granules from two mice were measured), more electron-lucent granules (Fig. 4E). The latter goblet cell granules are characteristic of those found in the normal mouse colon (Fig. 4F). Indeed, the differences in the appearance of these granules were sufficient to distinguish KO/Tg small intestine from control. Together, the transition in mucin subtypes and the altered ultrastructure of goblet cell granules suggest a colonic transformation of the KO/Tg small intestine.

Adult KO/Tg small intestine contains the same laminin isoforms as normal colon

As reduction in one laminin α chain can lead to compensatory changes in the expression of other related family members (Miner et al., 1998; Bolcato-Bellemin et al., 2003), we next assessed the deposition of laminin α chains in the KO/Tg small intestine. In the control, the BM underlying the villus epithelium contained primarily α5, with less detectable α1 and no α4 (Fig. 5A,C,E). In the absence of α5, laminins α1 and α4 accumulated ectopically in the villus subepithelial BM (Fig. 5B,D,F). We did not observe any alterations in laminin composition in the crypt subepithelial BM (Fig. 5), and there were no apparent changes in laminin α2 and α3 in the KO/Tg small intestine (data not shown). Therefore, given that laminin β1 is the major β chain and laminin γ1 the major γ1 chain in the intestinal subepithelial BM, the KO/Tg small intestine contains primarily laminin-111 (LM-111; α1β1γ1) (Aumailley et al., 2005) and LM-411 (α4β1γ1) rather than LM-511 in the villus subepithelial BM. Additional immunohistochemical studies demonstrated that nidogen-1, type IV collagen, and perlecan were deposited appropriately in the KO/Tg small intestine (data not shown). Ultrastructural analysis of the KO/Tg subepithelial BM did not reveal any differences from control (data not shown). Thus, increased expression of laminin α1 and/or α4 likely compensates for the loss of α5 by maintaining the integrity of the BM. Interestingly, similar laminin isoform compensation occurred in the *Lama5*$^{-/-}$ embryonic intestinal graft (Fig. S3).

The colonic transformation of the KO/Tg small intestine led us to hypothesize that normal colonic BMs should contain less LM-511 but more LM-111 and LM-411 as compared to small intestinal villi. Indeed, compared to villus BMs, laminin α5 was expressed at very low levels in the colonic epithelial BMs, except for those that are immediately underneath the surface epithelium (Fig. 5G,H). In addition, by immunostaining, high levels of laminins α1 and α4 were detected in the colonic epithelial BM (Fig. 5I-L). This distribution is similar to the small intestinal villus BM of KO/Tg mice, but opposite to that observed in WT small intestine (Fig. 5). Thus, mouse small intestine and colon normally contain different laminins, and the laminin composition in KO/Tg small intestine has switched from a small intestinal type (primarily LM-511) to a colonic type (primarily LM-111 and LM-411). And because this switch preceded the morphological changes in the KO/Tg small intestine, our data suggest that the identity of laminins in the subepithelial BM provides instructions for patterning the intestinal mucosa, either towards small intestinal crypt-villus units or towards colonic crypt-surface units.

Adult KO/Tg mice display aberrant epithelial cell behavior in the small intestine

To gain insights into the cellular mechanisms that underlie tissue patterning and remodeling in the KO/Tg small intestine, we examined cell proliferation, migration, differentiation and apoptosis in these mice. Cellular phenotypes from relatively normal looking KO/Tg villi were studied to try to avoid any phenotypes potentially secondary to morphological changes in the villi.

Proliferation—Immunofluorescence using antibodies directed against Ki67, an antigen expressed in proliferating cells, showed a statistically significant 1.5 fold increase on average in the length of the proliferative compartment in the KO/Tg small intestine compared to control

(4 mice per group, 10 crypts measured per mouse; $P<0.001$) (Fig. 6A,B,G). An alternative method, labeling of proliferating cells with 5-bromodeoxyuridine (BrdU), revealed a 1.6 fold increase on average in the number of proliferating cells per crypt in the KO/Tg small intestine (4 mice per group, 20 crypts analyzed per mouse; $P<0.001$).

Migration—We initially assayed intestinal epithelial cell migration up the villus by administering a single intraperitoneal injection of BrdU and analyzing the position of BrdU-labeled cells 24 hours later. After 24 hours, the leading edge of BrdU-labeled KO/Tg enterocytes was typically within 5-10 cells of the villus tip (in well oriented sections), whereas the leading edge of the BrdU-positive enterocytes in Het/Tg mice was only 3-5 cells from the crypt opening (Fig. 6C,D). Quantification of the distance from the crypt-villus junction to the top BrdU-positive cell revealed that KO/Tg epithelial cells migrate significantly faster than control cells (Fig. 6H). This finding was validated in one pair of mice by performing a staggered chlorodeoxyuridine (CldU)/iododeoxyuridine (IdU) double labeling experiment in which the distance that cells migrated after exit from the crypt in 12 hours was calculated by measuring the distance between the highest CldU-labeled cell and the highest IdU-labeled cell on the same villus (Fig. 6E,F). The KO/Tg epithelial cells migrated significantly faster than Het/Tg cells, at a rate of about 6 μm/hour, versus 3 μm/hour for the control (35 villi measured from each mouse; $P<0.001$).

Differentiation—We next investigated whether KO/Tg epithelial cells exhibited proper differentiation along the four intestinal epithelial lineages. Immunostaining for sucrase-isomaltase, a marker for differentiated enterocytes in the distal small intestine, did not reveal any difference between KO/Tg and Het/Tg, even in morphologically disturbed villi (Fig. 6I-K). Similarly, there was no difference in sucrase-isomaltase at the mRNA level (Fig. 6L). Immunostaining for chromogranin A, a marker for enteroendocrine cells, showed that the number and distribution of this cell type were similar in KO/Tg and controls (Fig. S4A,B). In contrast, there appeared to be elevated numbers of Paneth cells and goblet cells in the KO/Tg small intestine, based on immunostaining for lysozyme and periodic acid-Schiff stain, respectively (Fig. S4C-F).

In addition to cell lineage-specific marker changes, at both light and electron microscope levels we noted a conspicuous population of cells in the KO/Tg small intestine that were intermediate in appearance between goblet and Paneth cells (Fig. 6M-O). Such intermediate cells can occasionally be observed at crypt-villus junctions in wild-type small intestine, and they likely represent the common progenitor cells of the goblet and Paneth cell lineages (Troughton and Trier, 1969; Kamal et al., 2001). In KO/Tg mice, the number of intermediate cells was dramatically increased (Fig. 6P), and these cells were ectopically located either on sides of villi or at the bases of crypts, where only terminally differentiated cells should be found (Fig. 6N and data not shown).

Apoptosis—We investigated whether the apoptosis rate was altered in the KO/Tg small intestine by counting the number of cells with apoptotic bodies in H&E-stained paraffin sections. In four KO/Tg-Het/Tg littermate pairs at various ages, there were no significant differences in apoptosis noted either in the crypts or on the villi (data not shown). The increase in proliferation without a concomitant increase in apoptosis may be responsible in part for the observed lengthening of the crypts.

Lutheran, a cell surface receptor for laminin α5, is down-regulated in KO/Tg small intestine

To investigate the molecular mechanisms whereby laminins regulate intestinal epithelial cell behavior, we examined the localization and expression levels of known laminin receptors, including integrin α3β1, α6β1, α6β4, dystroglycan, and the Lutheran blood group glycoprotein/

basal cell adhesion molecule (Lu/B-CAM) (Miner and Yurchenco, 2004). By immunostaining, we did not find any significant changes in integrin α3,α6, β1, β4, or dystroglycan in the KO/Tg small intestine (Fig. S5). Immunostaining with an antibody specifically recognizing the activated form of integrin β1 also did not reveal any changes, suggesting that activation of β1-containing integrins is not impacted by the altered BM composition (Fig. S5). Immunostaining for Lu/B-CAM revealed that it is expressed at relatively low levels in the intestinal mucosa compared to the intestinal smooth muscle. In the mucosa, Lu was highly expressed in the mesenchymal structures in the villus core, but only extremely weak expression was found at the basal surface of the intestinal epithelial cells (Fig. 7A). This basal staining was never observed in the KO/Tg small intestine (Fig. 7B). Lutheran expression at the basal surface was higher in the proximal small intestine, but this staining was reduced in KO/Tg mice (Fig. 7C,D).

$p27^{Kip1}$, a cell cycle inhibitor, is down-regulated in KO/Tg small intestine

The increased cell proliferation and reduced differentiation in KO/Tg mice prompted us to examine the localization and expression level of $p27^{Kip1}$, a cell-cycle inhibitor that is known to inhibit S phase entry, promote cell cycle exit, and maintain cells in a differentiated state (Tian and Quaroni, 1999; Kaldis, 2007). In control small intestine, $p27^{Kip1}$ expression was mainly localized to the nuclei of differentiated cells at the bottom of crypts and along the villi (Fig. 7E). In KO/Tg small intestine, the nuclear localization of $p27^{Kip1}$ was dramatically reduced (Fig. 7F); this was shown with two different antibodies in five pairs of mice.

Impaired lipid absorption in KO/Tg mice

The dramatic loss of distal small intestine surface area in the KO/Tg mice suggests that these mice should exhibit absorption defects, particularly in regard to lipids, which are normally absorbed in the distal small intestine. We assayed dietary lipid absorption by feeding control and KO/Tg mice a high-fat diet (21% fat by weight, 42% of calories from fat). Food intake and feces output were determined daily, and total fecal lipids were extracted and quantified. We found that feces from KO/Tg mice contained twice as much lipid as control mice (Table 2). This finding translates into a 3% reduction in lipid absorption in KO/Tg mice as compared to Het/Tg mice (n=3). These data suggest a functional deficit that reflects the morphological defects.

DISCUSSION

Lama5$^{-/-}$; Mr5 mice as a model to study the roles of laminins in intestinal morphogenesis

In the adult intestine, five different laminin isoforms (laminin-111, -211, -332, -411 and -511) predominate. Importantly, these isoforms are distributed in specific patterns along the crypt-villus axis of the intestine and are developmentally regulated ((Simon-Assmann et al., 1998; Lefebvre et al., 1999; Teller et al., 2007) and our study). Functional studies of laminins in the adult intestine have been hampered by early embryonic lethality or functional redundancy. Mice deficient for laminin α1, β1 or γ1 all die prior to E7, before intestinal development begins (Smyth et al., 1999; Miner et al., 2004; Alpy et al., 2005; Scheele et al., 2005). Even though laminin α2 or α4 deficient mice are able to survive to adulthood, no apparent intestinal defects are seen in these mice, perhaps due to compensation by laminin α1 (Simon-Assmann et al., 1994 and our unpublished data). Laminin α3 knockout mice die neonatally, and the intestinal phenotype has not been examined (Ryan et al., 1999). Laminin α5 knockout mice do not survive beyond E17; they exhibit smooth muscle defects in the embryonic small intestine, but no obvious alterations in villus organization were reported (Miner et al., 1998; Bolcato-Bellemin et al., 2003). Here, *Lama5*$^{-/-}$; Mr5 mice represent a mouse model in which laminin α5 deposition is specifically lost in the subepithelial BM of the small intestine in postnatal mice. A similar model cannot be conveniently created using a conditional knockout strategy, as laminin α5 in

the small intestine is secreted by both epithelial and mesenchymal cells (Lefebvre et al., 1999; Bolcato-Bellemin et al., 2003). Therefore, common small intestine-specific Cre transgenes, such as Fabp-cre or villin-cre, which are only expressed by epithelial cells, should not effectively eliminate laminin α5 from the subepithelial BM.

In vivo and in vitro functions of laminins in intestinal epithelial cells

The dramatic alterations in cell proliferation, migration and differentiation in KO/Tg mice are consistent with in vitro data showing that different laminin isoforms exhibit distinct properties in regulating these and other processes. We were unable to delineate individual contributions from each laminin isoform in vivo due to the nature of compensation by laminin family members. Our data do suggest that laminins, in the context of the BM, regulate tissue patterning and remodeling by fine-tuning intestinal epithelial cell behavior. The crypt restricted deposition of laminin α2 is consistent with its function in promoting cell proliferation in vitro (Dowgiert et al., 2004). The abrupt onset of laminin α5 deposition at the crypt-villus junction and its abundance in the villus subepithelial BM suggest a role in inducing cell differentiation. In the absence of laminin α5, the proliferative compartment expanded, suggesting a delay in initiating differentiation, despite the up-regulation of α1 and α4. Enterocytes differentiated normally in the absence of laminin α5, likely due to up-regulation of laminin α1, as α1 has been shown to induce Caco2 cell differentiation into mature enterocyte-like cells (Turck et al., 2005). However, the terminal differentiation of goblet cells was affected by the absence of laminin α5 and/or the increased expression of laminin α1 and α4, as shown by the increased numbers of intermediate cells and alteration of mucous granules towards the colon type. Finally, the faster cell migration observed in KO/Tg small intestine could result from the combined reduction in laminin α5 and the increased α4 in the subepithelial BM, because LM-511 was found to be the most adhesive substrate in vitro compared to other isoforms (Siler et al., 2000; Pouliot et al., 2002; Turck et al., 2005), and LM-411 potently promotes cell migration (Fujiwara et al., 2001). Further studies will be needed to confirm these proposed functions for laminin isoforms.

Laminins as regulators of tissue patterning

The gastrointestinal tube is regionalized into stomach, small intestine and colon with distinct patterns of mucosal folding. This regionalization is governed by a combination of signaling molecules and transcription factors (Rossant and Tam, 2002; Kerszberg and Wolpert, 2007). We have now provided evidence that laminins serve as positional cues during the regionalization of the intestinal tube into small intestine and colon. We showed that mouse small intestine and colon normally contain different combinations of laminin isoforms; a transition in laminin composition from a small intestinal type to a colonic type leads to remodeling of small intestinal mucosa to a colon-like mucosa. In addition, our grafting experiments suggest that the correct combination of laminin isoforms is also required for patterning the small intestinal mucosa during early postnatal development.

Laminin exhibits several features that make it an attractive candidate to provide positional information. 1) There are over 15 different laminin heterotrimers identified so far (Miner and Yurchenco, 2004), and combinations of these isoforms create even more heterogeneity, accommodating the need for multiple patterns. 2) Different laminin isoforms have distinct effects on cell proliferation, differentiation, migration, and likely apoptosis (Vachon and Beaulieu, 1995; Siler et al., 2000; Pouliot et al., 2002; Turck et al., 2005). The combination of various isoforms could therefore facilitate the fine-tuning required for specific tissue patterns. 3) BMs are widely distributed in the body, surrounding all epithelia, endothelia, muscles, fat cells and peripheral nerves (Kalluri, 2003). Therefore, a similar mechanism specifying position can be used in various contexts. Furthermore, laminins might cooperate with morphogens, either directly by binding and sequestering or concentrating them (Blaess et al., 2004), or

indirectly via effects on BM heparan sulfate proteoglycans (Steer et al., 2004), to increase the precision of positional specification.

Cell signaling downstream of laminins

It is important to address the interactions between laminins and cell surface receptors in order to understand the mechanism of laminin functions. Integrin α3β1, α6β1, α6β4, and dystroglycan are common and well-studied receptors for laminins (Miner and Yurchenco, 2004). Mice lacking the integrin β4 cytoplasmic domain die at birth and exhibit reduced proliferation in the small intestine (Murgia et al., 1998). In contrast, conditional knockout of integrin β1 in the small intestine leads to increased epithelial proliferation through regulation of hedgehog signaling (Jones et al., 2006). That deletions of two receptors for laminins exert opposite effects in the intestinal epithelium suggests that the regulation of intestinal epithelial cell behavior by laminins is complex. We did not find changes in the expression or localization of integrins in KO/Tg mice, and despite considerable efforts, found no consistent changes in the focal adhesion kinase (FAK) or phosphoinositol-3-kinase (PI3K) pathways downstream. However, these results do not exclude the possibility that there are alterations in integrin signaling that may be impossible to discern with available methods. Lu/B-CAM is another laminin receptor, and laminin α5 is its only known extracellular matrix ligand (Moulson et al., 2001; Parsons et al., 2001; Kikkawa et al., 2002)). As Lu/B-CAM knockout mice do not exhibit a villus coalescence phenotype (Rahuel et al., 2008) and our own unpublished observations), it is unlikely that the reduction in Lu/B-CAM expression/localization that we observed in the KO/Tg small intestine is relevant to the aberrant intestinal patterning.

$p27^{Kip1}$ is a cyclin-dependent kinase (CDK) inhibitor that negatively regulates cell cycle progression (Sherr and Roberts, 1999). Besides this well-known role, recent studies suggest that $p27^{Kip1}$ also regulates other aspects of cellular behavior, including differentiation and migration, and possibly apoptosis (Coqueret, 2003; Kawauchi et al., 2006; Nguyen et al., 2006; Itoh et al., 2007). $p27^{Kip1}$ is normally expressed in the small intestine at the crypt-villus junction and within villi, overlapping with the deposition pattern of laminin α5 in the adjacent BM. In the KO/Tg small intestine, there was a dramatic reduction of $p27^{Kip1}$ nuclear localization associated with the reduction of laminin α5. These data raise the interesting possibility that cellular defects observed in KO/Tg mice are mediated, at least partially, by the loss of nuclear localization of $p27^{Kip1}$. Future work will be necessary to link the regulation of $p27^{Kip1}$ to laminin, and to address whether the altered $p27^{Kip1}$ levels in KO/Tg small intestine are responsible for defective cell proliferation, differentiation, and/or migration.

In summary, using a knockout/transgenic rescue strategy, we generated mice containing reduced laminin α5 and elevated laminin α1 and α4 in the subepithelial BM of the small intestine. The KO/Tg small intestine displayed a laminin composition similar to normal colon. This laminin switch affected the nuclear localization of $p27^{Kip1}$ and altered the homeostasis of small intestinal epithelial cells, which subsequently led to the remodeling of the KO/Tg distal small intestinal mucosa to a more posterior, colon-like mucosa. Our study has revealed a previously unrecognized instructive role for laminins in patterning the mouse gut tube.

MATERIALS AND METHODS

Generation and genotyping of *Lama5* knockout and Mr5 transgenic mice

The generation and characterization of *Lama5*$^{-/-}$ and full length laminin α5 (Mr5) transgenic mice have been described (Miner et al., 1998; Moulson et al., 2001). Mice were maintained on a mixed 129-C57BL/6J-CBA/J background. Studies were approved by the Washington University Animal Studies Committee. For genotyping, DNA extracted from tail biopsies was amplified by PCR using the following primer pairs to detect the three alleles:

Lama5 (+): 5’-GGAGTCTGTATCTGGCATCTG-3’ and 5’-CACAATCTGCAGAAGGTGTGG-3’;

Lama5 (-): 5’-CGCTTGACCTTGGACATAGCTGG-3’ and 5’-GCGATTAAGTTGGGTAACGCC-3’;

Mr5: 5’-TCTAGAGCGCATCACGCAGG-3’ and 5’-CCATGAGGTGGCCCAGTAGC-3’.

Antibodies, immunostaining and histology

The following antibodies and reagents were used: rat anti-laminin α1 and β1 (Abrahamson et al., 1989; St John et al., 2001) (clones 8B3 and 5A2, respectively, gifts from Dale Abrahamson, University of Kansas Medical Center, Kansas City, KS); rat anti-laminin α2 (Schuler and Sorokin, 1995) (clone 4H8-2, Alexis Biochemicals/Axxora); rabbit anti-LM-332 (Marinkovich et al., 1992) (a gift from M. Peter Marinkovich, Stanford University, Stanford, CA); rabbit anti-laminin α4 (Sasaki et al., 2001) and anti-Lutheran (gifts from Takako Sasaki, Portland, OR); rabbit anti-laminin α5 (Miner et al., 1997); rat anti-laminin γ1 (MAB1914, Chemicon); rabbit anti-sucrase isomaltase (a gift from Kwo-yih Yeh, Louisiana State University Health Sciences Center, Shreveport, LA); rabbit anti-chromogranin A (ImmunoStar); rabbit anti-lysozyme (LabVision); rabbit anti-Ki67 (Novocastra); mouse anti-BrdU (BD Biosciences); rabbit anti-integrin α3 (a gift from C. Michael Dipersio, Albany Medical College, Albany, NY); rat anti-integrin α6 (Chemicon); rat anti-integrin β1 (Chemicon); rat anti-integrin β4 (BD Pharmingen); mouse anti-dystroglycan (clone 7D11, Developmental Studies Hybridoma Bank); rat anti-activated integrin β1 (9EG7; BD Pharmingen); rabbit anti-$p27^{Kip1}$ (Zymed); mouse anti-$p27^{Kip1}$ (BD Biosciences); Hoechst 33342 (Sigma); Alexa488-conjugated anti-mouse IgG1 (Molecular Probes); FITC-conjugated anti-rat and Cy3-conjugated anti-rabbit (Chemicon).

For cryo-sections, mouse small intestine and colon were prepared as reported (Stappenbeck et al., 2002). Briefly, intestines were dissected and flushed with ice-cold PBS, pH=7.4, to remove the luminal contents. The lumen was then infused with OCT compound (VWR) prior to freezing in 2-methylbutane cooled in a dry ice-ethanol bath. Frozen sections were cut at 7 μm in a cryostat and air dried on gelatin-coated slides.

To prepare paraffin tissue sections, intestines were removed and flushed first with ice-old PBS, then with ice-cold 4% PFA in PBS. The intestines were then opened up along the mesenteric side, pinned on wax villus-side up, and fixed in 4% PFA in PBS at 4°C for 4-6 hours. After rinsing in PBS and dehydration in graded ethanols, the intestines were oriented in 2% agar prior to paraffin embedding. 5 μm-thick sections were cut parallel to either the cephalocaudal axis or the crypt-villus axis.

For scanning electron microscopy, 4 × 4 mm tissue fragments were fixed in 2% PFA/2.5% gluteraldehyde in 0.1M cacodylate buffer and post-fixed in 1% osmium tetroxide. After rinsing in H_2O, the tissue was treated with 1% thiocarbohydrazide, post-fixed with 0.1% osmium tetroxide, dehydrated in ethanol, and critical-point dried before being sputter coated with gold/palladium.

Immunostaining and transmission electron microscopy were carried out as described previously (Kikkawa et al., 2003). Immunostained sections were examined through a microscope equipped for epifluorescence (Eclipse E800; Nikon). Images were captured with a Spot 2 cooled color digital camera (Diagnostic Instruments) using Spot Software Version 3.5.9. Digital electron microscopic images were captured using a Hitachi H7500 transmission electron microscope or a Hitachi S-3000H scanning electron microscope. Images were imported into Adobe Photoshop 7.0 for processing and layout.

Intestinal epithelial cells isolation and real-time RT-PCR

Intact intestinal epithelia were isolated similarly as described (Bjerknes and Cheng, 1999). Briefly, mice were anesthetized and the intestinal lumen was flushed in situ with Calcium Magnesium Free Hanks Balanced Salt Solution (CMF-HBSS) to remove fecal contents. After intraventricular perfusion of 30 mM EDTA in CMF-HBSS, the intestines were everted and slipped onto a glass rod. The loosened intestinal epithelium was collected into ice-cold CMF-HBSS through vibration. Aliquots of the intestinal epithelial isolates were stained with trypan blue to assay cell viability, and the remainders were used for RNA isolation.

Total RNA was extracted from isolated intestinal epithelium or from scraped mucosa using TRI Reagent (Molecular Research Center), treated with DNA-free kit (Applied Biosystems/Ambion), and reverse-transcribed using SuperScript III First-Strand Synthesis System for RT-PCR (Invitrogen). Real-time PCR was carried out on each sample in triplicate on an ABI 7000 Real-time PCR system (Applied Biosystems) using SYBR Green PCR Master Mix (Applied Biosystems) and the following primer pairs:

Lama5: 5'-TGCCTCCTCCAAGAGGGATTGTTT-3' and 5'-TTCGCGAGTATTCTGTGGTGCAGA-3';

Gapdh: 5'-TGGCAAAGTGGAGATTGTTGCC-3' and 5'-AAGATGGTGATGGGCTTCCCG-3'.

Determination of intestinal epithelial cell migration rate

The CldU/IdU double labeling method utilizes two different BrdU monoclonal antibodies with different affinities for CldU and IdU. With this method (detailed in Vega and Peterson, 2005), CldU-labeled cells and IdU-labeled cells can be discriminated using rat anti-BrdU (BU1/75 ICR1, Abcam) and mouse anti-BrdU (clone B44, BD biosciences), respectively, with no cross-reactivity. *Lama5+/-;* Mr5 mice were labeled with CldU and IdU for 36 and 24 hours, respectively. *Lama5-/-;* Mr5 mice were labeled with CldU and IdU for 24 and 12 hours, respectively. These timings were chosen to ensure linear measurements of cell migration on the villi. The distance migrated in 12 hours was calculated as the distance between the first CldU-labeled cell and the first IdU-labeled cell.

High iron diamine staining

High iron diamine staining was performed as described previously (Spicer, 1965; Sheehan, 1980) with minor modification. Briefly, intestinal sections were deparaffinized, rehydrated, and then immersed overnight (24 hours) in high iron diamine solution, which contains 120 mg of *N*,*N*-dimethyl-*m*-phenylenediamine dihydrochloride and 20 mg of *N*,*N*-dimethyl-p-phenylenediamine hydrochloride dissolved in 50mL distilled water and then mixed with 1.4 ml of fresh 60% (wt/vol) ferric chloride. After washing in running water, sections were stained with 1% alcian blue in 3% acetic acid (pH=2.5) for 5 minutes and counterstained with 0.5% aqueous neutral red for 2-3 minutes. After washing in running water, sections were dehydrated, cleared, and mounted.

Lipid absorption analysis

Mice were maintained on a high fat western diet (Harlan) for three weeks before being transferred to individual metabolic cages to allow collection of feces and measurement of food consumption. Fecal lipid content and lipid absorption were measured as described previously (Newberry et al., 2006).

Statistical analyses

Two-tailed, unequal-variance *Student*'s *t*-tests were used throughout this study for determining statistical significance.

Supplementary Material

Refer to Web version on PubMed Central for supplementary material.

Acknowledgements

We thank Jeanette Cunningham, Gloriosa Go, Jennifer Richardson, and Cong Li for technical assistance; Dale Abrahamson, Peter Marinkovich, Takako Sasaki, Rupert Timpl, and Kwo-yih Yeh for antibodies; the Pulmonary Morphology Core (supported by NIH P01HL029594) and the Digestive Diseases Research Core Center Morphology Core (supported by NIH P30DK052574) for histology services; the Microscopy and Digital Imaging Core in the Research Center for Auditory and Vestibular Studies (supported by NIH P30DC004665) and the Washington University Center for Kidney Disease Research (supported by NIH P30DK079333) for electron microscopy support; and Brent Polk for helpful insights. Mice were housed in a facility supported by NIH grant C06RR015502. This work was supported by grants from the NIH (R01GM060432 and R01DK064687) and the March of Dimes (#1-FY02-192) to JHM. JHM is an Established Investigator of the American Heart Association.

References

Abrahamson DR, Irwin MH, St John PL, Perry EW, Accavitti MA, Heck LW, Couchman JR. Selective immunoreactivities of kidney basement membranes to monoclonal antibodies against laminin: localization of the end of the long arm and the short arms to discrete microdomains. J Cell Biol 1989;109:3477–3491. [PubMed: 2480964]

Alpy F, Jivkov I, Sorokin L, Klein A, Arnold C, Huss Y, Kedinger M, Simon-Assmann P, Lefebvre O. Generation of a conditionally null allele of the laminin alpha1 gene. Genesis 2005;43:59–70. [PubMed: 16100707]

Aumailley M, Bruckner-Tuderman L, Carter WG, Deutzmann R, Edgar D, Ekblom P, Engel J, Engvall E, Hohenester E, Jones JCR, et al. A simplified laminin nomenclature. Matrix Biol 2005;24:326–332. [PubMed: 15979864]

Bjerknes M, Cheng H. Colossal crypts bordering colon adenomas in Apc(Min) mice express full-length Apc. Am J Pathol 1999;154:1831–1834. [PubMed: 10362808]

Blaess S, Graus-Porta D, Belvindrah R, Radakovits R, Pons S, Littlewood-Evans A, Senften M, Guo H, Li Y, Miner JH, et al. Beta1-integrins are critical for cerebellar granule cell precursor proliferation. J Neurosci 2004;24:3402–3412. [PubMed: 15056720]

Bolcato-Bellemin AL, Lefebvre O, Arnold C, Sorokin L, Miner JH, Kedinger M, Simon-Assmann P. Laminin alpha5 chain is required for intestinal smooth muscle development. Dev Biol 2003;260:376–390. [PubMed: 12921739]

Booth C, Potten CS. Gut instincts: thoughts on intestinal epithelial stem cells. J Clin Invest 2000;105:1493–1499. [PubMed: 10841502]

Coqueret O. New roles for p21 and p27 cell-cycle inhibitors: a function for each cell compartment? Trends Cell Biol 2003;13:65–70. [PubMed: 12559756]

Deplancke B, Hristova KR, Oakley HA, McCracken VJ, Aminov R, Mackie RI, Gaskins HR. Molecular ecological analysis of the succession and diversity of sulfate-reducing bacteria in the mouse gastrointestinal tract. Appl Environ Microbiol 2000;66:2166–2174. [PubMed: 10788396]

Di Tonno F, Cassaro M, Bertoldin R, Vianello F, Di Pietro R, Lavelli D, Rugge M. Colonic metaplasia in the long-term follow-up of the ileal neobladder. Eur Urol 2001;39(Suppl 2):15–18. [PubMed: 11223691]

Dowgiert J, Sosne G, Kurpakus-Wheater M. Laminin-2 stimulates the proliferation of epithelial cells in a conjunctival epithelial cell line. Cell Prolif 2004;37:161–175. [PubMed: 15030550]

Fujiwara H, Kikkawa Y, Sanzen N, Sekiguchi K. Purification and characterization of human laminin-8. Laminin-8 stimulates cell adhesion and migration through alpha3beta1 and alpha6beta1 integrins. J Biol Chem 2001;276:17550–17558. [PubMed: 11278628]

Fukumoto S, Miner JH, Ida H, Fukumoto E, Yuasa K, Miyazaki H, Hoffman MP, Yamada Y. Laminin alpha5 is required for dental epithelium growth and polarity and the development of tooth bud and shape. J Biol Chem 2006;281:5008–5016. [PubMed: 16365040]

Itoh Y, Masuyama N, Nakayama K, Nakayama KI, Gotoh Y. The cyclin-dependent kinase inhibitors p57 and p27 regulate neuronal migration in the developing mouse neocortex. J Biol Chem 2007;282:390–396. [PubMed: 17092932]

Jones RG, Li X, Gray PD, Kuang J, Clayton F, Samowitz WS, Madison BB, Gumucio DL, Kuwada SK. Conditional deletion of beta1 integrins in the intestinal epithelium causes a loss of Hedgehog expression, intestinal hyperplasia, and early postnatal lethality. J Cell Biol 2006;175:505–514. [PubMed: 17088430]

Kaldis P. Another piece of the p27Kip1 puzzle. Cell 2007;128:241–244. [PubMed: 17254963]

Kalluri R. Basement membranes: structure, assembly and role in tumour angiogenesis. Nat Rev Cancer 2003;3:422–433. [PubMed: 12778132]

Kamal M, Wakelin D, Ouellette AJ, Smith A, Podolsky DK, Mahida YR. Mucosal T cells regulate Paneth and intermediate cell numbers in the small intestine of T. spiralis-infected mice. Clin Exp Immunol 2001;126:117–125. [PubMed: 11678907]

Kawauchi T, Chihama K, Nabeshima Y, Hoshino M. Cdk5 phosphorylates and stabilizes p27kip1 contributing to actin organization and cortical neuronal migration. Nat Cell Biol 2006;8:17–26. [PubMed: 16341208]

Kerszberg M, Wolpert L. Specifying positional information in the embryo: looking beyond morphogens. Cell 2007;130:205–209. [PubMed: 17662932]

Kikkawa Y, Miner JH. Molecular dissection of laminin alpha 5 in vivo reveals separable domain-specific roles in embryonic development and kidney function. Dev Biol 2006;296:265–277. [PubMed: 16750824]

Kikkawa Y, Virtanen I, Miner JH. Mesangial cells organize the glomerular capillaries by adhering to the G domain of laminin alpha5 in the glomerular basement membrane. J Cell Biol 2003;161:187–196. [PubMed: 12682087]

Kikkawa Y, Moulson CL, Virtanen I, Miner JH. Identification of the binding site for the Lutheran blood group glycoprotein on laminin a5 through expression of chimeric laminin chains in vivo. J Biol Chem 2002;277:44864–44869. [PubMed: 12244066]

Lefebvre O, Sorokin L, Kedinger M, Simon-Assmann P. Developmental expression and cellular origin of the laminin alpha2, alpha4, and alpha5 chains in the intestine. Dev Biol 1999;210:135–150. [PubMed: 10364433]

Marinkovich MP, Lunstrum GP, Burgeson RE. The anchoring filament protein kalinin is synthesized and secreted as a high molecular weight precursor. J Biol Chem 1992;267:17900–17906. [PubMed: 1517226]

Mimura T, Kuramoto S, Yamasaki K, Kaminishi M. Familial adenomatous polyposis: a case report and histologic mucin study. J Clin Gastroenterol 1999;28:372–376. [PubMed: 10372942]

Miner JH. Developmental biology of glomerular basement membrane components. Curr Opin Nephrol Hypertens 1998;7:13–19. [PubMed: 9442357]

Miner JH, Li C. Defective glomerulogenesis in the absence of laminin α5 demonstrates a developmental role for the kidney glomerular basement membrane. Dev Biol 2000;217:278–289. [PubMed: 10625553]

Miner JH, Yurchenco PD. Laminin functions in tissue morphogenesis. Annu Rev Cell Dev Biol 2004;20:255–284. [PubMed: 15473841]

Miner JH, Cunningham J, Sanes JR. Roles for laminin in embryogenesis: exencephaly, syndactyly, and placentopathy in mice lacking the laminin alpha5 chain. J Cell Biol 1998;143:1713–1723. [PubMed: 9852162]

Miner JH, Li C, Mudd JL, Go G, Sutherland AE. Compositional and structural requirements for laminin and basement membranes during mouse embryo implantation and gastrulation. Development 2004;131:2247–2256. [PubMed: 15102706]

Miner JH, Patton BL, Lentz SI, Gilbert DJ, Snider WD, Jenkins NA, Copeland NG, Sanes JR. The laminin alpha chains: expression, developmental transitions, and chromosomal locations of alpha1-5,

identification of heterotrimeric laminins 8-11, and cloning of a novel alpha3 isoform. J Cell Biol 1997;137:685–701. [PubMed: 9151674]

Moulson CL, Li C, Miner JH. Localization of Lutheran, a novel laminin receptor, in normal, knockout, and transgenic mice suggests an interaction with laminin alpha5 in vivo. Dev Dyn 2001;222:101–114. [PubMed: 11507772]

Moulson CL, Lin MH, White JM, Newberry EP, Davidson NO, Miner JH. Keratinocyte-specific expression of fatty acid transport protein 4 rescues the wrinkle-free phenotype in Slc27a4/Fatp4 mutant mice. J Biol Chem 2007;282:15912–15920. [PubMed: 17401141]

Murgia C, Blaikie P, Kim N, Dans M, Petrie HT, Giancotti FG. Cell cycle and adhesion defects in mice carrying a targeted deletion of the integrin beta4 cytoplasmic domain. Embo J 1998;17:3940–3951. [PubMed: 9670011]

Newberry EP, Xie Y, Kennedy SM, Luo J, Davidson NO. Protection against Western diet-induced obesity and hepatic steatosis in liver fatty acid-binding protein knockout mice. Hepatology 2006;44:1191–1205. [PubMed: 17058218]

Nguyen L, Besson A, Heng JI, Schuurmans C, Teboul L, Parras C, Philpott A, Roberts JM, Guillemot F. p27kip1 independently promotes neuronal differentiation and migration in the cerebral cortex. Genes Dev 2006;20:1511–1524. [PubMed: 16705040]

Nguyen NM, Miner JH, Pierce RA, Senior RM. Laminin alpha5 is required for lobar septation and visceral pleural basement membrane formation in the developing mouse lung. Dev Biol 2002;246:231–244. [PubMed: 12051813]

Parsons SF, Lee G, Spring FA, Willig TN, Peters LL, Gimm JA, Tanner MJ, Mohandas N, Anstee DJ, Chasis JA. Lutheran blood group glycoprotein and its newly characterized mouse homologue specifically bind alpha5 chain-containing human laminin with high affinity. Blood 2001;97:312–320. [PubMed: 11133776]

Potten CS, Booth C, Pritchard DM. The intestinal epithelial stem cell: the mucosal governor. Int J Exp Pathol 1997;78:219–243. [PubMed: 9505935]

Pouliot N, Saunders NA, Kaur P. Laminin 10/11: an alternative adhesive ligand for epidermal keratinocytes with a functional role in promoting proliferation and migration. Exp Dermatol 2002;11:387–397. [PubMed: 12366691]

Radtke F, Clevers H. Self-renewal and cancer of the gut: two sides of a coin. Science 2005;307:1904–1909. [PubMed: 15790842]

Rahuel C, Filipe A, Ritie L, El Nemer W, Patey-Mariaud N, Eladari D, Cartron JP, Simon-Assmann P, Le Van Kim C, Colin Y. Genetic inactivation of the laminin alpha5 chain receptor Lu/BCAM leads to kidney and intestinal abnormalities in the mouse. Am J Physiol Renal Physiol 2008;294:F393–406. [PubMed: 18032551]

Rebustini IT, Patel VN, Stewart JS, Layvey A, Georges-Labouesse E, Miner JH, Hoffman MP. Laminin alpha5 is necessary for submandibular gland epithelial morphogenesis and influences FGFR expression through beta1 integrin signaling. Dev Biol 2007;308:15–29. [PubMed: 17601529]

Rossant, J.; Tam, PPL. Mouse development : patterning, morphogenesis, and organogenesis. San Diego, Calif.: Academic Press; 2002.

Ryan MC, Lee K, Miyashita Y, Carter WG. Targeted disruption of the LAMA3 gene in mice reveals abnormalities in survival and late stage differentiation of epithelial cells. J Cell Biol 1999;145:1309–1323. [PubMed: 10366601]

Sancho E, Batlle E, Clevers H. Signaling pathways in intestinal development and cancer. Annu Rev Cell Dev Biol 2004;20:695–723. [PubMed: 15473857]

Sasaki T, Mann K, Timpl R. Modification of the laminin alpha 4 chain by chondroitin sulfate attachment to its N-terminal domain. FEBS Lett 2001;505:173–178. [PubMed: 11557064]

Scheele S, Falk M, Franzen A, Ellin F, Ferletta M, Lonaio P, Andersson B, Timpl R, Forsberg E, Ekblom P. Laminin alpha1 globular domains 4-5 induce fetal development but are not vital for embryonic basement membrane assembly. Proc Natl Acad Sci U S A 2005;102:1502–1506. [PubMed: 15668394]

Schuler F, Sorokin LM. Expression of laminin isoforms in mouse myogenic cells in vitro and in vivo. J Cell Sci 1995;108:3795–3805. [PubMed: 8719886]

Sheehan, DC. Theory and Practice of Histotechnology. C. V. Mosby; 1980.

Sherr CJ, Roberts JM. CDK inhibitors: positive and negative regulators of G1-phase progression. Genes Dev 1999;13:1501–1512. [PubMed: 10385618]

Siler U, Seiffert M, Puch S, Richards A, Torok-Storb B, Muller CA, Sorokin L, Klein G. Characterization and functional analysis of laminin isoforms in human bone marrow. Blood 2000;96:4194–4203. [PubMed: 11110691]

Simon-Assmann P, Turck N, Sidhoum-Jenny M, Gradwohl G, Kedinger M. In vitro models of intestinal epithelial cell differentiation. Cell Biol Toxicol 2007;23:241–256. [PubMed: 17171431]

Simon-Assmann P, Lefebvre O, Bellissent-Waydelich A, Olsen J, Orian-Rousseau V, De Arcangelis A. The laminins: role in intestinal morphogenesis and differentiation. Ann N Y Acad Sci 1998;859:46–64. [PubMed: 9928369]

Simon-Assmann P, Duclos B, Orian-Rousseau V, Arnold C, Mathelin C, Engvall E, Kedinger M. Differential expression of laminin isoforms and alpha 6-beta 4 integrin subunits in the developing human and mouse intestine. Dev Dyn 1994;201:71–85. [PubMed: 7803849]

Smyth N, Vatansever HS, Murray P, Meyer M, Frie C, Paulsson M, Edgar D. Absence of Basement Membranes after Targeting the LAMC1 Gene Results in Embryonic Lethality Due to Failure of Endoderm Differentiation. J Cell Biol 1999;144:151–160. [PubMed: 9885251]

Spicer SS. Diamine Methods for Differentialing Mucosubstances Histochemically. J Histochem Cytochem 1965;13:211–234. [PubMed: 14327695]

St John PL, Wang R, Yin Y, Miner JH, Robert B, Abrahamson DR. Glomerular laminin isoform transitions: errors in metanephric culture are corrected by grafting. Am J Physiol Renal Physiol 2001;280:F695–705. [PubMed: 11249861]

Stappenbeck TS, Wong MH, Saam JR, Mysorekar IU, Gordon JI. Notes from some crypt watchers: regulation of renewal in the mouse intestinal epithelium. Curr Opin Cell Biol 1998;10:702–709. [PubMed: 9914172]

Stappenbeck TS, Hooper LV, Manchester JK, Wong MH, Gordon JI. Laser capture microdissection of mouse intestine: characterizing mRNA and protein expression, and profiling intermediary metabolism in specified cell populations. Methods Enzymol 2002;356:167–196. [PubMed: 12418197]

Steer DL, Shah MM, Bush KT, Stuart RO, Sampogna RV, Meyer TN, Schwesinger C, Bai X, Esko JD, Nigam SK. Regulation of ureteric bud branching morphogenesis by sulfated proteoglycans in the developing kidney. Dev Biol 2004;272:310–327. [PubMed: 15282150]

Suemori H, Kadodawa Y, Goto K, Araki I, Kondoh H, Nakatsuji N. A mouse embryonic stem cell line showing pluripotency of differentiation in early embryos and ubiquitous beta-galactosidase expression. Cell Differ Dev 1990;29:181–186. [PubMed: 2112419]

Teller IC, Auclair J, Herring E, Gauthier R, Menard D, Beaulieu JF. Laminins in the developing and adult human small intestine: relation with the functional absorptive unit. Dev Dyn 2007;236:1980–1990. [PubMed: 17503455]

Tian JQ, Quaroni A. Involvement of p21(WAF1/Cip1) and p27(Kip1) in intestinal epithelial cell differentiation. Am J Physiol 1999;276:C1245–1258. [PubMed: 10362586]

Timpl R. Macromolecular organization of basement membranes. Curr Opin Cell Biol 1996;8:618–624. [PubMed: 8939648]

Timpl R, Brown JC. Supramolecular assembly of basement membranes. BioEssays 1996;18:123–132. [PubMed: 8851045]

Troughton WD, Trier JS. Paneth and goblet cell renewal in mouse duodenal crypts. J Cell Biol 1969;41:251–268. [PubMed: 5775788]

Turck N, Gross I, Gendry P, Stutzmann J, Freund JN, Kedinger M, Simon-Assmann P, Launay JF. Laminin isoforms: biological roles and effects on the intracellular distribution of nuclear proteins in intestinal epithelial cells. Exp Cell Res 2005;303:494–503. [PubMed: 15652360]

Vachon PH, Beaulieu JF. Extracellular heterotrimeric laminin promotes differentiation in human enterocytes. Am J Physiol 1995;268:G857–867. [PubMed: 7539221]

Vega CJ, Peterson DA. Stem cell proliferative history in tissue revealed by temporal halogenated thymidine analog discrimination. Nat Methods 2005;2:167–169. [PubMed: 15782184]

Yurchenco PD, Amenta PS, Patton BL. Basement membrane assembly, stability and activities observed through a developmental lens. Matrix Biol 2004;22:521–538. [PubMed: 14996432]

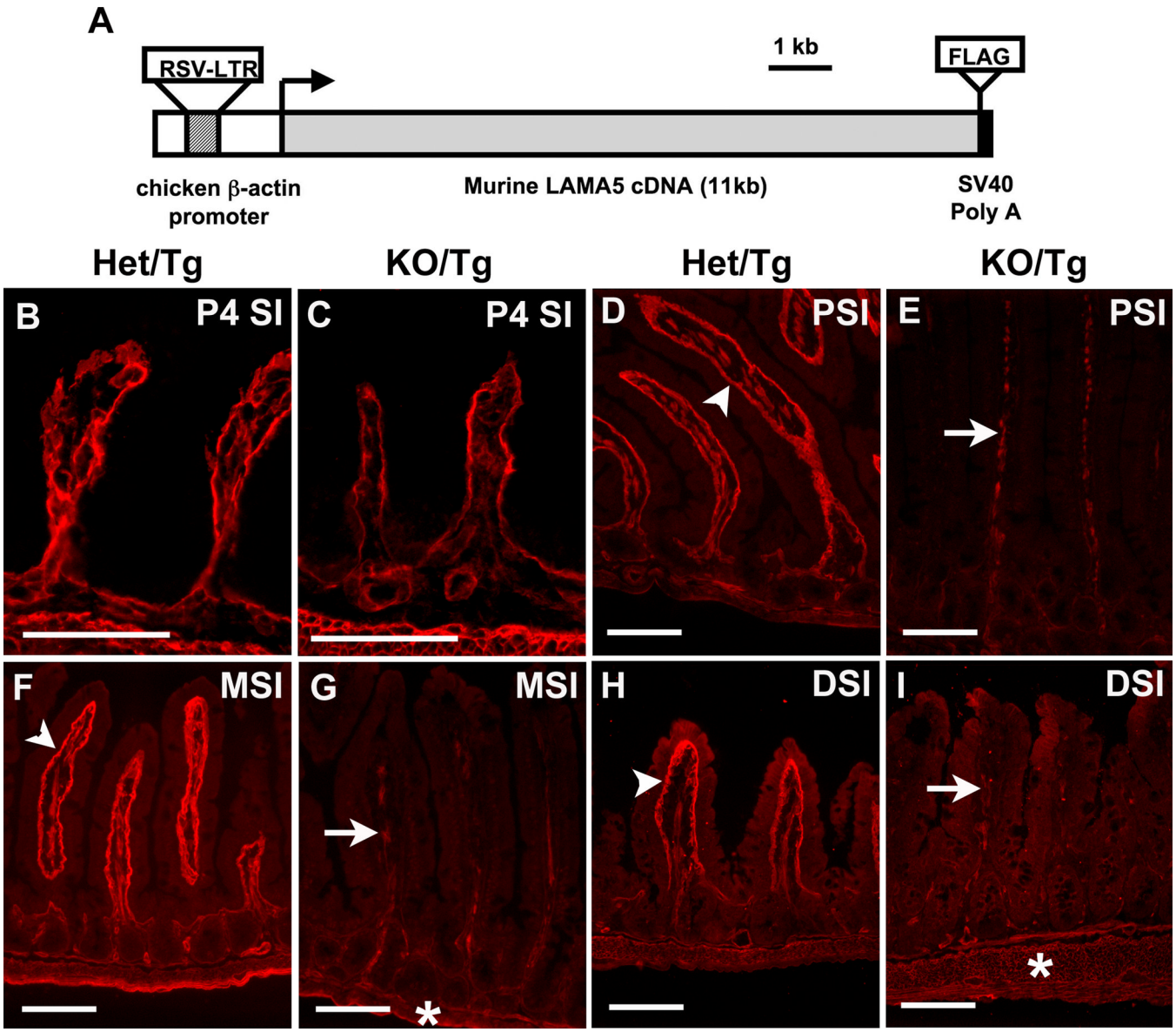

Figure 1. Laminin α5 is greatly reduced in the small intestine of postnatal KO/Tg mice

(A) Schematic diagram of the Mr5 transgene. (B,C) Frozen sections of small intestine from newborn Het/Tg (B) and KO/Tg (C) mice. Immunostaining for laminin α5 revealed similar levels in the epithelial (inner) BM. (D-I) Representative pictures of laminin α5 staining in the proximal (PSI), middle (MSI) and distal (DSI) small intestine of adult mice. (D,F,H) Laminin α5 was abundantly deposited in the subepithelial BM of control villi (denoted by arrowhead), with almost none in the crypts. (E,G,I) Laminin α5 was greatly reduced in the villus BM of KO/Tg mice but was detectable in mesenchymal structures within villi (arrows) and in intestinal smooth muscle (asterisk) of both Het/Tg and KO/Tg mice. Bars, 100 μm.

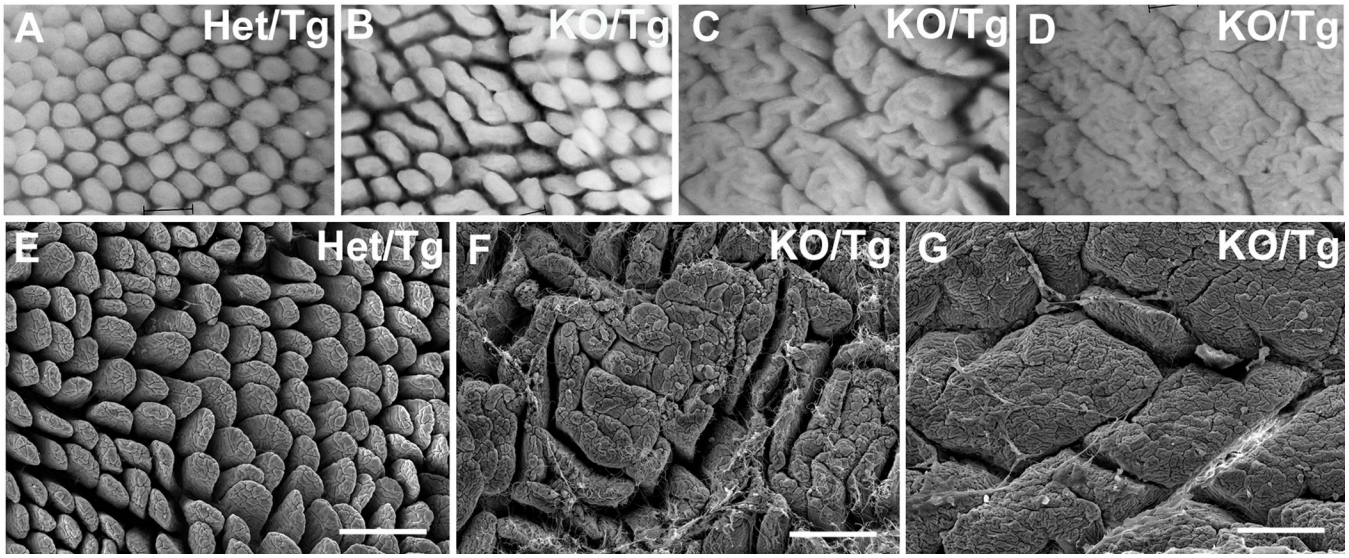

Figure 2. Villus coalescence in adult KO/Tg distal small intestine

(A-D) Whole mount views of distal small intestinal mucosa. Compared to the villi of Het/Tg mice (A), the KO/Tg villi (B-D) showed varying degrees of villus coalescence, from a widened phenotype (B) to a “cerebroid” pattern (C) to a “mosaic” pattern (D). (E-G) Scanning electron micrographs confirmed the findings in (A-D). Bars, 200 μm.

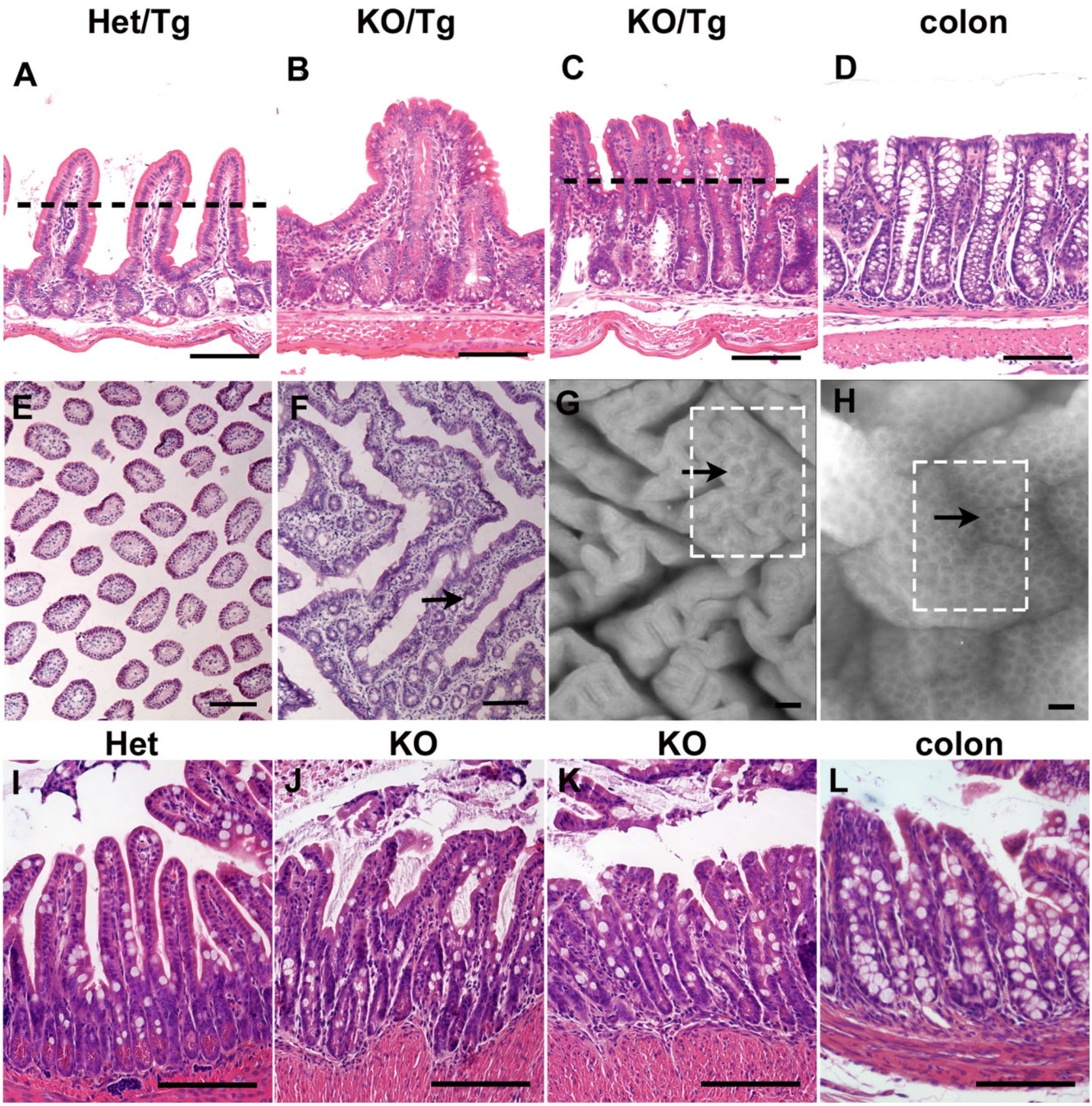

Figure 3. Crypt-villus architecture is disrupted in adult KO/Tg distal small intestine

(A-C) H&E stained sections of distal small intestines. KO/Tg showed varying degrees of loss of normal crypt-villus architecture (A-C) and resembled colon (D). (E, F) Villus coalescence was clearly seen in cross sections. Note the crypt-like structures trapped in the center (arrow in F). The approximate positions of cross-sectioning are indicated by dashed lines in A and C. (G,H) Whole mount views of intestinal mucosa. KO/Tg small intestine (G) develops local flat epithelial surfaces (boxed area) with visible crypt mouths (arrow) that were also observed in normal colon (arrow and boxed area in H). (I-L) H&E stained sections of intestinal grafts. *Lama5*$^{-/-}$ small intestinal grafts (J,K) failed to develop a normal crypt-villus architecture (I) but instead presented a colon-like architecture (L). Bars, 100 μm.

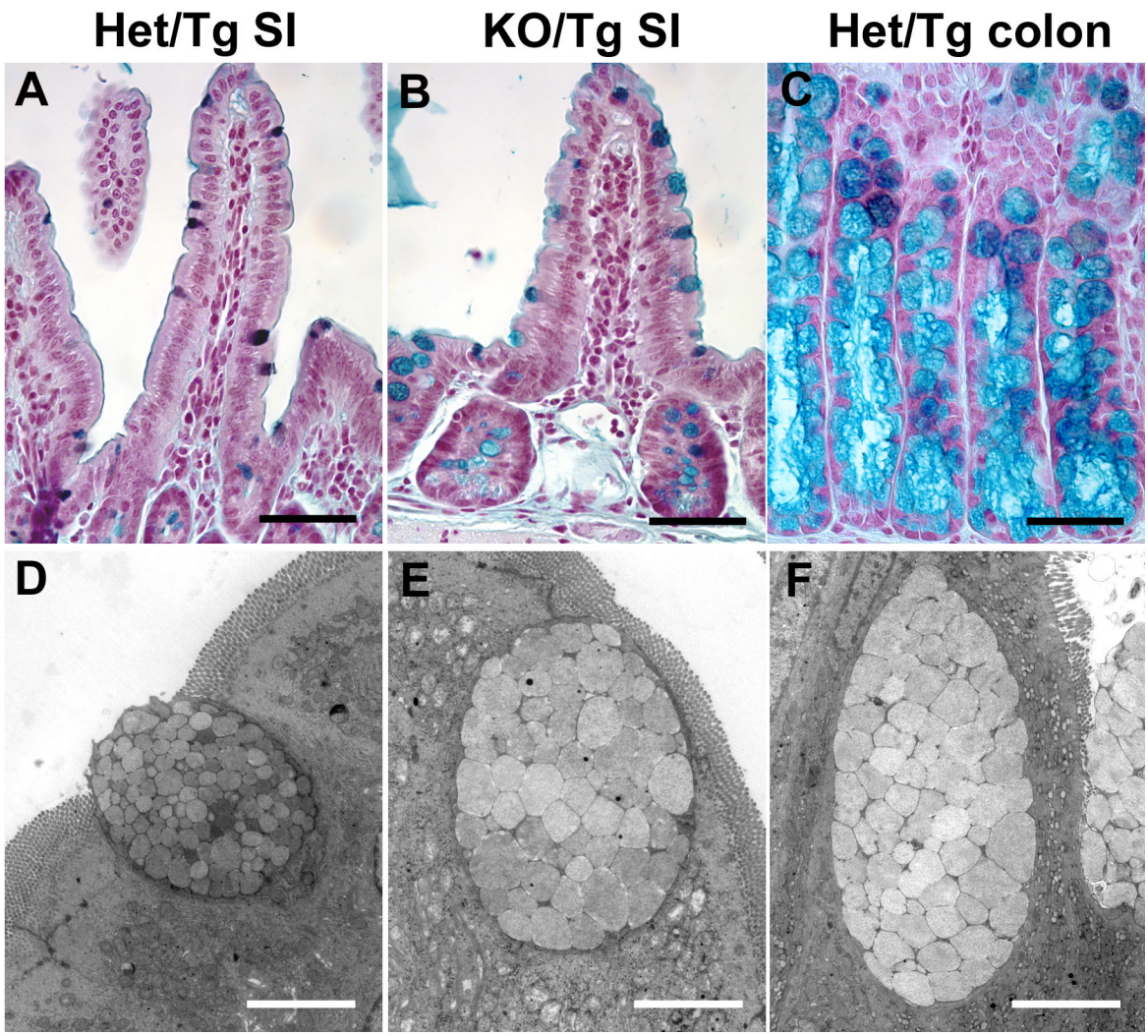

Figure 4. KO/Tg distal small intestines lose small intestinal features and exhibit characteristics of colon

(A-C) High iron diamine staining of intestine. Most control distal small intestine goblet cells contained sulfomucin (dark brown in A), whereas most KO/Tg distal small intestine goblet cells contained sialomucin (blue in B), which is characteristic of colonic goblet cells (blue in C). (D-F) Transmission electron micrographs of goblet cells. The goblet cell in the KO/Tg distal small intestine (E) and wild-type colon (F) are similar; both contain larger and more electron lucent granules than those in goblet cells from normal distal small intestine (D). Bars, 50 μm (A-C); 4 μm (D-F).

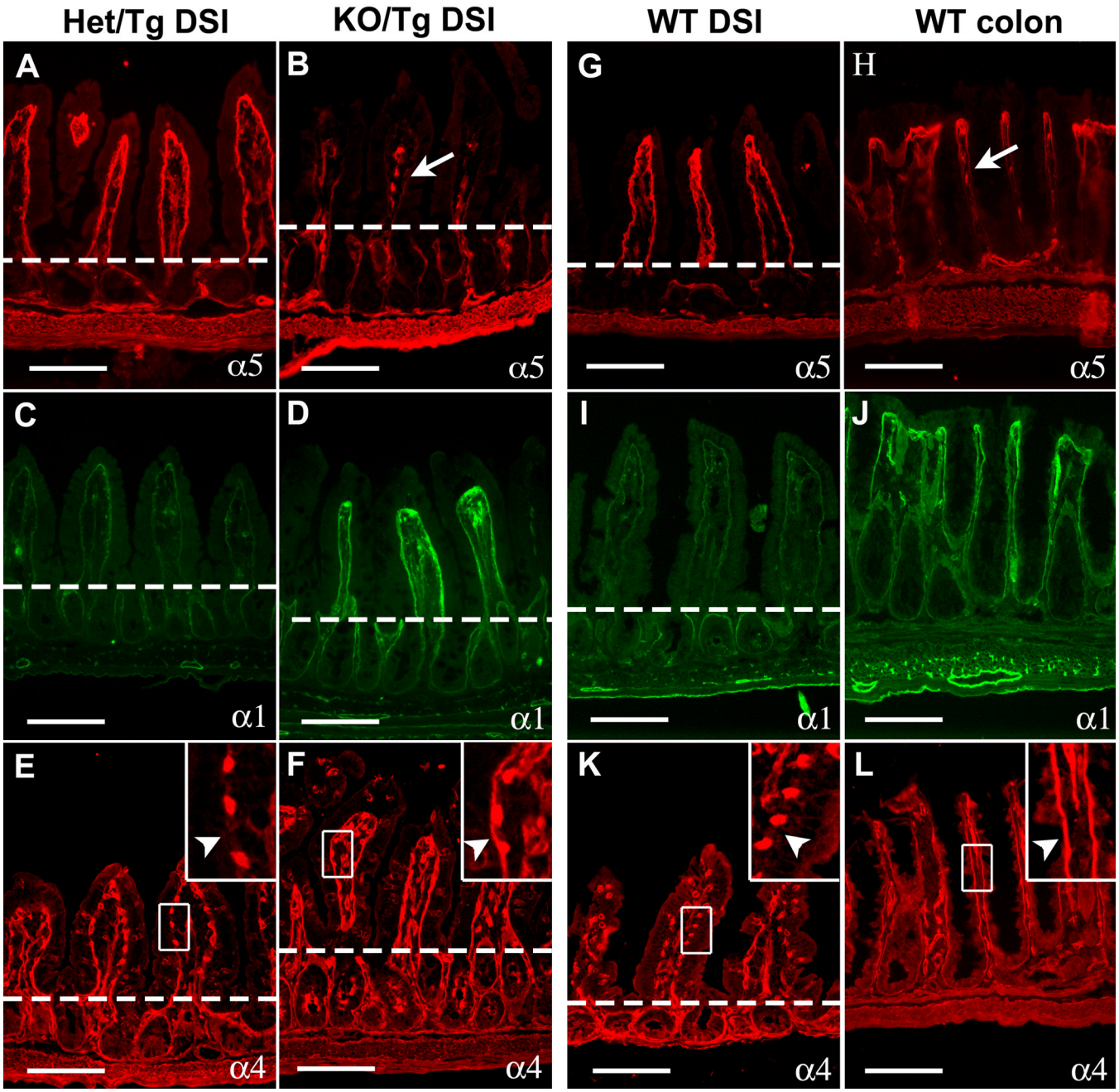

Figure 5. The laminin composition of KO/Tg small intestinal subepithelial BMs resembles that of the normal colon

Intestine sections were stained with antisera directed against laminin α chains, as indicated. The dashed lines denote the crypt-villus boundary. (A) α5 was detected in the control subepithelial BM of villi but not of crypts. (B) α5 staining was greatly reduced in villus BM (arrow) of KO/Tg mice but was detectable in both the mesenchymal structures within villi and the intestinal smooth muscle wall. (C) Low levels of α1 were detected in the control subepithelial BMs of both villi and crypts. (D) Levels of α1 were increased in KO/Tg villus BM. (E) In controls, high levels of α4 were detected in the endothelial BM of blood vessels, but not in the villus subepithelial BM (arrowhead in inset). (F) In KO/Tg, in addition to endothelial BM, α4 was deposited in the villus subepithelial BM (arrowhead in inset). (G-L)

Compared to WT distal small intestine, α5 was only weakly deposited in the subepithelial BMs of WT colon (arrow in H), whereas α1 and α4 were abundant. Bars=100 μm.

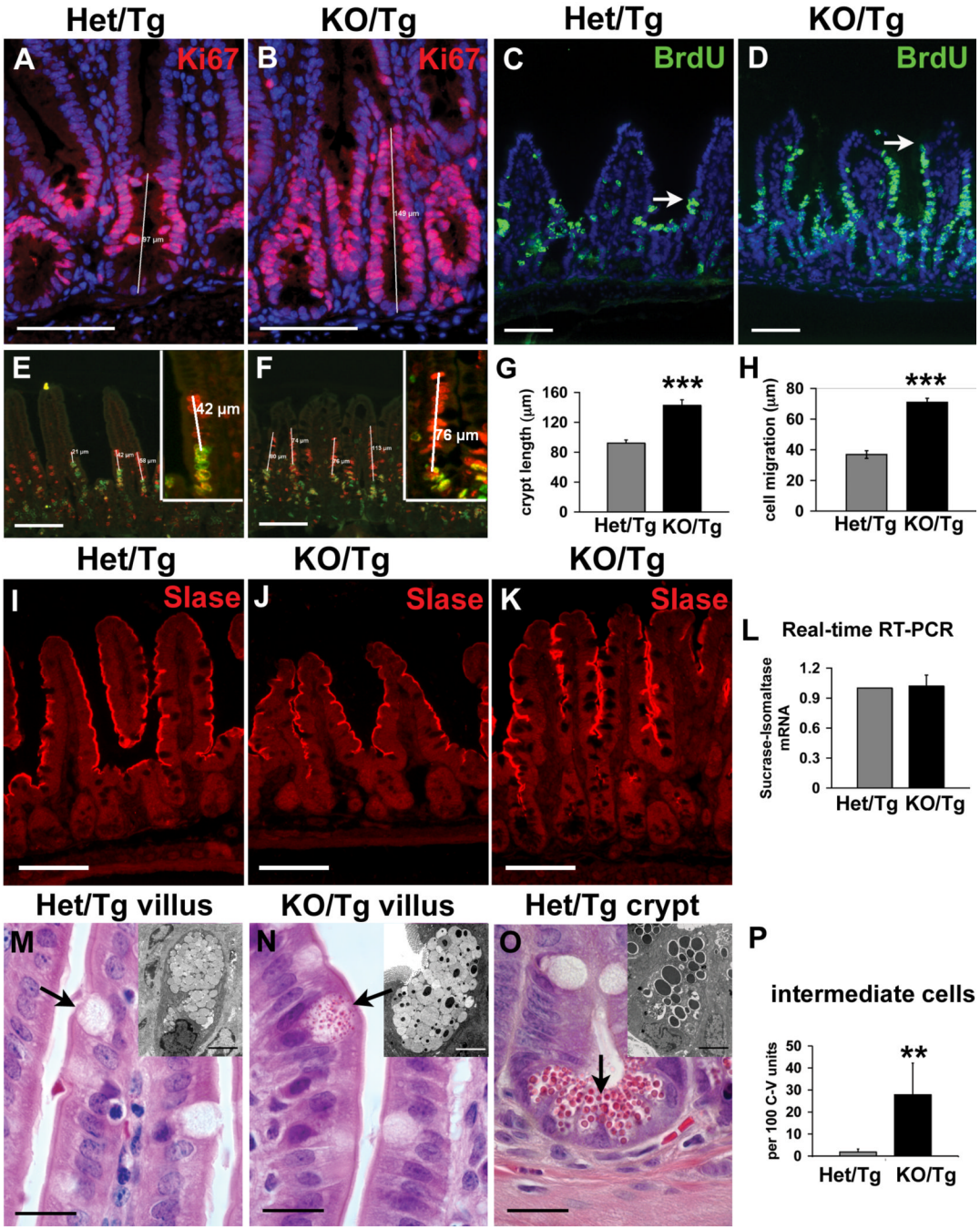

Figure 6. Intestinal epithelial cell behavior is altered in KO/Tg small intestines

(A,B) Sections of distal small intestines from Het/Tg and KO/Tg mice stained with anti-Ki67 (red; Hoechst labels all nuclei blue) shows the expanded proliferative compartment in KO/Tg mice; this result is quantified in G (4 mice per group, 10 crypts measured per mouse; $P<0.001$). (C,D) Staining for BrdU (green) 24 hours after BrdU injection shows that KO/Tg intestinal epithelial cells migrated much farther up villi than did controls; arrows denote the leading edge of BrdU-positive cells. This is quantified in H (4 mice per group, 32 villi measured per mouse; $P<0.001$). (E,F) CldU (red) and IdU (green) staining. The distance between the leading edge of the CldU-labeled and the IdU-labeled epithelial cells is the distance migrated during the 12 hours between CldU and IdU injections. (I-K) Sections of distal small intestines from Het/Tg

and KO/Tg mice stained with an antibody against Sucrase-Isomaltase (SIase). SIase expression was similar in Het/Tg and KO/Tg. (L) Quantification of SIase mRNA levels in small intestine using real-time RT-PCR (n=4, P=0.85). Values shown are fold changes normalized to results from Het/Tg. (M-O) H&E staining of paraffin sections revealed “intermediate” cells on KO/Tg villi (arrow in N). These cells contained apical eosinophilic granules smaller than those in mature Paneth cells (arrow in O) and were absent from controls (arrow in M). The insets in M-O are transmission electron micrographs of granules from a normal goblet cell (M), an intermediate cell (N), and a normal Paneth cell (O). Intermediate cells contain both electron lucent granules as seen in Het/Tg goblet cells (M) and electron-dense granules as seen in Paneth cells (O). (P) Quantification of intermediate cells per 100 crypt-villus units in Het/Tg and KO/Tg distal small intestine (4 mice/group, 200 crypt-villus units quantified/mouse; P=0.006). Bar, 100μm in A-F, I-K; 20 μm in M-O; and 4 μm in the insets of M-O. In graphs, the error bars indicate SEMs. Triple asterisks: P<0.001; double asterisks: P<0.01.

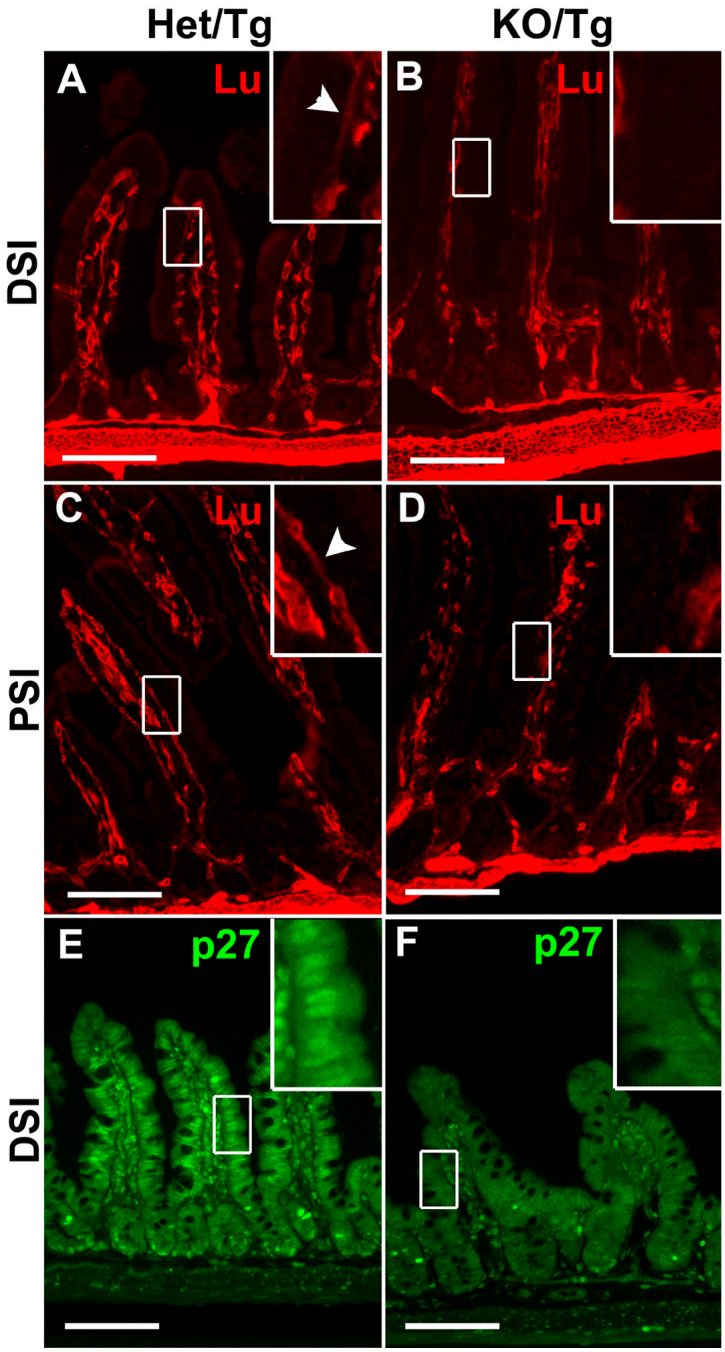

Figure 7. Reduced Lutheran expression and p27^{Kip1} nuclear localization in KO/Tg distal small intestine

(A-D) Sections of distal small intestines (A,B) and proximal small intestines (C,D) from Het/Tg and KO/Tg mice were stained with an antibody against Lutheran. Lutheran expression was high in smooth muscle, medium in the villus core, and very low at the basal surface of intestinal epithelial cells in the Het/Tg DSI (A and inset). Lutheran expression in the villus core and at the basal surface of intestinal epithelial cells was reduced in the KO/Tg DSI (B and inset). Lutheran was detected at higher levels on the basal surface of intestinal epithelial cells in Het/Tg PSI than Het/Tg DSI (A,C and insets), and this expression was reduced in the KO/Tg PSI (D and inset). Arrowheads in (A,C) point to the basal expression of Lutheran. (E,F) Sections

of distal small intestines were stained with an antibody against $p27^{Kip1}$. $p27^{Kip1}$ was detected in the nuclei of differentiated intestinal epithelial cells at the bottom of crypts and on the villi in Het/Tg small intestine (E and inset). Nuclear staining was dramatically reduced in KO/Tg distal small intestine (F and inset). Bars=100 μm.

Table 1

Lama5 mRNA levels are reduced in KO/Tg small intestine.

Age	RNA source	Het/Tg $\Delta C_T \pm s$	KO/Tg $\Delta C_T \pm s$	Average fold change (range)
1 month	scraped mucosa	11.03±0.16	13.54±0.13	-5.7 (-5.2 to -6.2)
6 month	isolated intestinal epithelial cells	12.35±0.12	19.66±0.16	-158.7 (-142.0 to -177.3)
10 month	isolated intestinal epithelial cells	12.01±0.31	19.05±0.18	-131.6 (-116.2 to -149.1)

s = standard deviation of the ΔC_T value.

Table 2

Lama5-/-; Mr5 mice absorb less dietary lipid compared to controls.

	Het/Tg	KO/Tg	
lipid content in feces	5.2%	10%	$p<0.05$ n=3
% of lipid absorption	98%	95%	$p<0.05$ n=3